

Path integral calculation for emergence of rapid evolution from demographic stochasticity

Hong-Yan Shih and Nigel Goldenfeld

*Department of Physics, Center for the Physics of Living Cells and Institute for Genomic Biology,
University of Illinois at Urbana-Champaign, Loomis Laboratory of Physics,
1110 West Green Street, Urbana, Illinois, 61801-3080*

Genetic variation in a population can sometimes arise so fast as to modify ecosystem dynamics. Such phenomena have been observed in natural predator-prey systems, and characterized in the laboratory as showing unusual phase relationships in population dynamics, including a π phase shift between predator and prey (evolutionary cycles) and even undetectable prey oscillations compared to those of the predator (cryptic cycles). Here we present a generic individual-level stochastic model of interacting populations that includes a subpopulation of low nutritional value to the predator. Using a master equation formalism, and by mapping to a coherent state path integral solved by a system-size expansion, we show that evolutionary and cryptic quasi-cycles can emerge generically from the combination of intrinsic demographic fluctuations and clonal mutations alone, without additional biological mechanisms.

PACS numbers: 87.23.-n, 87.18.Tt, 05.40.-a, 02.50.Ey

Predator-prey ecosystems exhibit noisy population oscillations whose origin is intuitively quite clear. The predator population number is activated by the prey, and so increases. This in turn inhibits the growth of the prey population, but the decline of the prey leads to a corresponding decline in the predator number too. As a result the prey population begins to rise, and the cycle begins again. The simplicity of this narrative belies the difficulty of making a quantitative model of ecosystems. Strong demographic fluctuations degrade the utility of population-level modeling, rendering it problematic to assess the appropriate scales for ecological modeling [1–6]. For example, observations of noisy periodicity in time series [7], slowly-decaying correlations [8] and spatiotemporal patterns [9] clearly reflect the stochastic nature of populations [10, 11] and their spatial organization. Moreover, even the simplest predator-prey systems exhibit complex spatial structure. This can arise through a variety of pattern formation processes [12–16] that include recent results on deterministic [17, 18] and fluctuation-induced Turing instabilities [9, 19, 20], traveling waves [16, 21, 22] and even analogies to the processes of phase separation in binary alloys [23]. In short, collective and stochastic many-body phenomena are ubiquitous in biology, and perhaps nowhere more so than in ecology.

A major conceptual advance was the development of individual-level models (ILM), which used statistical mechanics to capture demographic stochasticity and derive population-level dynamics from a microscopic description of organismal interactions for both well-mixed [24, 25] and spatially-extended predator-prey ecosystems [19, 20, 26, 27]. This advance takes explicit account of the discrete nature of individuals in a population, and uses a system-size expansion [28] of the master equation to show how demographic noise acts as a driver of number fluctuations: in a sense, the shot noise persistently drives decaying population fluctuations, whose overall effect is

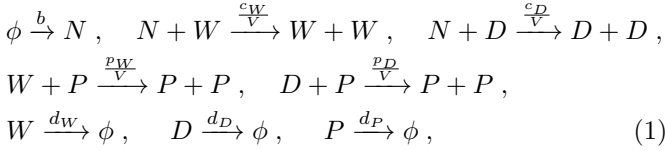
to produce noisy but periodic population dynamics and spatial patterns. A natural way to formulate these phenomena, especially in a spatially-extended context, is to adapt the annihilation and creation operators of field theory to this classical context [29–32] (for a review and history, see Ref. ([33])), and thence to derive a path-integral formulation that is especially convenient for calculation [20, 27, 34].

The classical literature on predator-prey systems [35] assumes that evolution occurs on such long time scales that it can be neglected, but it is not obvious that this is always valid [36]. Recent work using rotifers (predator) and algae (prey) in a chemostat shows that dramatic changes in the population structure of the rotifer-algae predator-prey system can arise from rapid responses to intense selection among induced genetically distinct strains [37–44]. In these studies, so-called subpopulations with different traits emerge from evolution and lead to new trophic structures, accompanied by anomalous ecological dynamics. These anomalies include ‘evolutionary cycles’ with long oscillation periods in population dynamics and predator-prey phase shifts near π (and definitely distinct from the canonical value of $\pi/2$), and ‘cryptic cycles’, in which prey populations remain almost constant while the predator population oscillates. Such phenomena have been modeled with deterministic differential equations containing empirical descriptions of functional response with a variety of detailed hypotheses on the mechanism of species interactions [38–40, 43, 45–48]. It has also been proposed that non-heritable phenotypic plasticity of prey and predator could generate the observed anomalous phase relationships due to rapid adaptation [49, 50]. Such explanations are not only very complex, with many adjustable parameters, but also cannot address the stochasticity evident in the observations.

The purpose of this Letter is to study the effect of demographic stochasticity for rapid evolution in well-mixed systems. We propose a minimal stochastic individual-

level model (SILM) for rapid evolution which we solve analytically and by Gillespie simulation [51]. We show that this simple stochastic model can predict rapid evolution phenomena, yielding phase diagrams that are similar to those of more complex deterministic models and in qualitative agreement with available data. Our results imply that rapid evolution can be explained by subpopulation dynamics driven simply by intrinsic demographic stochasticity, without additional biological mechanisms.

ILM for rapid evolution:- First consider a model for a system composed of nutrients for the prey (N), the vulnerable (wild-type) prey (W), the so-called ‘defended’ (mutant) prey (D), and the predator (P). The basic individual processes for them are regrowth of nutrients, reproduction of prey, predation by predator and death for all species:



where ϕ denotes the vacuum state, and V is an effective coarse-grained volume in which the dynamics can be regarded as well-mixed. In ecology, this is called the patch size. Later we will examine the dynamics in the limit $V \rightarrow \infty$. Because of defense, the defended prey has a smaller predation rate by the predator than the wild-type prey, *i.e.* $p_D < p_W$, and also has a smaller reproduction rate due to the metabolic cost for defense, *i.e.* $c_W < c_D$. The corresponding master equation that defines the time evolution of the probability distribution of population states is

$$\begin{aligned} \partial_t P(\{n_i\}) &= \left[b(E_N^{-1} - 1)(n_{N,\max} - n_N) \right. \\ &\quad + \frac{c_j}{V}(E_N E_j^{-1} - 1)n_N n_j + \frac{p_j}{V}(E_j E_P^{-1} - 1)n_j n_P \\ &\quad \left. + d_j(E_j - 1)n_j + d_P(E_D - 1)n_P \right] P(\{n_i\}), \end{aligned} \quad (2)$$

where the prey index $j = W, D$ and E_i^{\pm} are the raising and lowering operators of population n_i for species $i = N, W, D, P$.

Coherent-state path integral formalism:- In this section we apply the Doi formalism [29] to map Eq. (2) to a second quantized Hamiltonian and a path integral. By introducing the probability state vector

$$|\psi\rangle = \sum_{\{n_i\}} P(\{n_i\}) |\{n_i\}\rangle, \quad (3)$$

the master equation automatically satisfies

$$\partial_t |\psi\rangle = -\hat{H} |\psi\rangle, \quad (4)$$

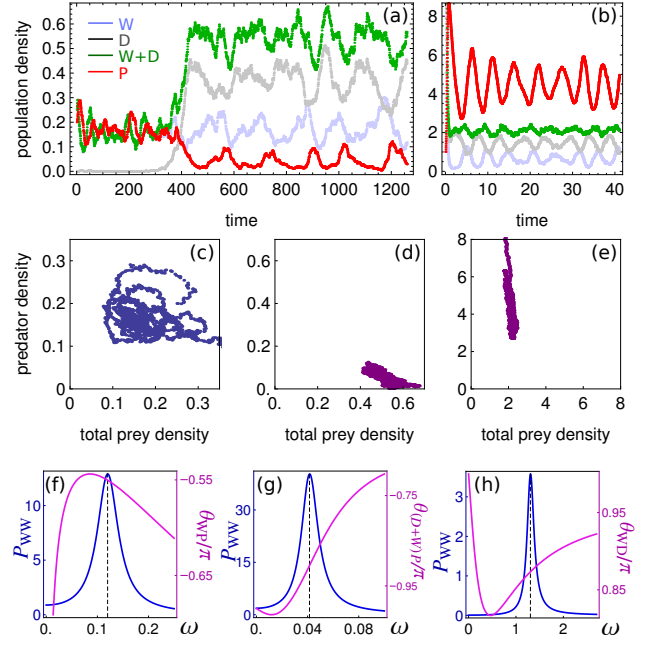


FIG. 1. Stochastic simulations for (a)evolutionary cycles emerging from normal cycles due to random mutation and for (b)cryptic cycles. Phase portraits of (c)normal cycles and (e)evolutionary cycles from the stochastic simulations show that the phase differences between predator and the total prey population are roughly $\pi/2$ and π respectively, while for (e)cryptic cycles there is no obvious phase relationship. The estimated phase differences from analytic calculations based on ILM are -0.55π and 0.905π for (f)normal cycles and (g)evolutionary cycles, and the predicted phase difference between the wild-type prey and the defended prey is approximately 0.874π . Parameter values are (a) $V = 1000$, $c_W = 0.3$, $p_W = 0.6$, $c_D/c_W = 0.8$, $p_D/p_W = 0.01$, $d_D/d_W = 1$, $\phi_{N,\max} = 1$, and $b = 0.1$; (b) $V = 380$, $c_W = 60$, $p_W = 0.92$, $c_D/c_W = 0.95$, $p_D/p_W = 0.001$, $d_D/d_W = 7.5$, $\phi_{N,\max} = 16$, and $b = 0.1$.

where

$$\begin{aligned} \hat{H} &= b \left(1 - \hat{a}_N^\dagger \right) \left(n_{N,\max} - \hat{a}_N^\dagger \hat{a}_N \right) + \frac{c_j}{V} \left[\hat{a}_N^\dagger \hat{a}_N \hat{a}_j^\dagger \hat{a}_j \right. \\ &\quad \left. - \hat{a}_N \left(\hat{a}_j^\dagger \right)^2 \hat{a}_j \right] + \frac{p_j}{V} \left[\hat{a}_j^\dagger \hat{a}_j \hat{a}_P^\dagger \hat{a}_P - \hat{a}_j \left(\hat{a}_P^\dagger \right)^2 \hat{a}_P \right] \\ &\quad + d_j \left(\hat{a}_j^\dagger \hat{a}_j - \hat{a}_j \right) + d_P \left(\hat{a}_P^\dagger \hat{a}_P - \hat{a}_P \right) \end{aligned}$$

By using the coherent-state representation, the Hamiltonian can be mapped onto the basis of coherent states and becomes a function of α_i^* and α_i which are the eigenstates of \hat{a}_i^\dagger and \hat{a}_i respectively. The corresponding Lagrangian density in the path integral form becomes

$$\mathcal{L} = \sum_i \alpha_i^* \partial_t \alpha_i + H(\{\alpha_i^*\}, \{\alpha_i\}) \quad (5)$$

It is convenient to map the system onto the physical basis by applying the semiclassical Cole-Hopf transformation [22]

$$\alpha_i^* = e^{\tilde{\rho}_i}, \quad \alpha_i = \rho_i e^{-\tilde{\rho}_i} \quad (6)$$

where ρ_i and $\tilde{\rho}_i$ are the mean-field population variables and fluctuation variables for species i . The Hamiltonian density under the transformation is obtained as

$$\begin{aligned} H = & b(1 - d\tilde{\rho}_N)(n_{N,\max} - \rho_N) + \frac{c_j}{V}(1 - e^{\tilde{\rho}_j - \tilde{\rho}_N}) \\ & + \frac{p_j}{V}(1 - e^{\tilde{\rho}_P - \tilde{\rho}_j}) + d_j\rho_j(1 - e^{-\tilde{\rho}_j}) \\ & + d_P\rho_P(1 - e^{-\tilde{\rho}_P}). \end{aligned} \quad (7)$$

Further we apply the ansatz that assumes the dominating noise is Gaussian [27]

$$\tilde{\rho}_i \rightarrow \frac{\tilde{\rho}_i}{\sqrt{V}}, \quad \rho_i = V\phi_i + \sqrt{V}\xi_i, \quad (8)$$

where $\langle \tilde{\rho}_i \rangle$ are the mean-field population density variables and the fluctuations around them, ϕ_i , are of order $1/\sqrt{V}$. However, it is important to emphasize that the Gaussian noise here should not be additive but is multiplicative because these fluctuations originate from the demographic stochasticity of the population at each time step, resulting quasicycles induced by a resonant amplification of intrinsic fluctuations [24] and leading to a longer tail in distribution distinct from the limit cycles [20]. After applying the expansion in Eq. (8), the Lagrangian in Eq. (5) can be separated into different orders of \sqrt{V}

$$\mathcal{L} = \sqrt{V}\mathcal{L}_1 + \mathcal{L}_2 + \dots \quad (9)$$

Here

$$\begin{aligned} \mathcal{L}_1 = & \sum_i \tilde{\rho}_i \partial_t \phi_i + b\phi_N \tilde{\rho}_N + c_j \phi_N \phi_j (\tilde{\rho}_N - \tilde{\rho}_j) \\ & + p_j \phi_j \phi_P (\tilde{\rho}_j - \tilde{\rho}_P) + d_j \phi_j \tilde{\rho}_j + d_P \phi_P \tilde{\rho}_P \end{aligned} \quad (10)$$

which gives the mean-field dynamics:

$$\frac{\delta \mathcal{L}_1}{\delta \tilde{\rho}_N} = \partial_t \phi_N - b(\phi_{N,\max} - \phi_N) + c_j \phi_N \phi_j = 0, \quad (11)$$

$$\frac{\delta \mathcal{L}_1}{\delta \tilde{\rho}_j} = \partial_t \phi_j - c_j \phi_N \phi_j + p_j \phi_j \phi_P - d_j \phi_j = 0, \quad (12)$$

$$\frac{\delta \mathcal{L}_1}{\delta \tilde{\rho}_P} = \partial_t \phi_P - p_j \phi_j \phi_P + d_P \phi_P = 0. \quad (13)$$

The leading fluctuation dynamics is described by

$$\mathcal{L}_2 = \tilde{\rho}^T \partial_t \xi - \tilde{\rho}^T \mathbf{A} \xi - \frac{1}{2} \tilde{\rho}^T \mathbf{B} \xi \quad (14)$$

where $\mathbf{f} = (f_N, f_W, f_D, f_P)$ for $f = \rho, \xi$, and $\mathbf{A}_{NN} = -b - c_j \phi_j$, $\mathbf{A}_{Nj} = -\mathbf{A}_{jN} = -c_j \phi_N$, $\mathbf{A}_{NP} = \mathbf{A}_{PN} = \mathbf{A}_{WD} = \mathbf{A}_{Dj} = 0$, $\mathbf{A}_{jj} = c_j \phi_j - p_j \phi_P - d_j$, $\mathbf{A}_{jP} = -\mathbf{A}_{Pj} = -p_j \phi_j$, $\mathbf{A}_{PP} = p_j \phi_j - d_P$ and $\mathbf{B}_{NN} = b(\phi_{N,\max} - \phi_N) + c_j \phi_N \phi_j$, $\mathbf{B}_{Nj} = \mathbf{B}_{jN} = -c_j \phi_N \phi_j$, $\mathbf{B}_{NP} = \mathbf{B}_{PN} = \mathbf{B}_{WD} = \mathbf{B}_{DW} = 0$, $\mathbf{B}_{jj} = c_j \phi_N \phi_j + p_j \phi_j \phi_P - d_j \phi_j$, $\mathbf{B}_{jP} = \mathbf{B}_{Pj} = -p_j \phi_j \phi_P$, $\mathbf{B}_{PP} = p_j \phi_j \phi_P - d_P \phi_P$.

Eq. (14) is equivalent to the Langevin equations

$$\frac{d\xi(t)}{dt} = \mathbf{A}\xi(t) + \gamma(t), \quad \langle \gamma_i(t) \gamma_j(t') \rangle = 2\pi \mathbf{B}_{ij} \delta(t - t'), \quad (15)$$

which describe the dynamics of demographic noise. Since the matrix \mathbf{A} is governed by the macroscopic densities, the demographic noise is multiplicative. Also, the Langevin equations in Eq. (15) are linear without the white noise γ , and thus the solutions for ξ contributed by the linear terms are expected to decay exponentially and converge to mean-field densities ϕ .

However, the multiplicative white noise plays an important role: whenever it can cancel out the contribution of the eigenvalues of \mathbf{A} , the dynamics of ξ will be driven away from convergent mean-field densities, *i.e.* white noise can select the frequency in the deterministic equations. This is interpreted as a resonant effect induced by stochastic noise [24].

Power spectrum, phase relationship and phase diagram. The power spectrum of demographic noise has a resonant frequency corresponding to the deterministic eigenvalue. The power spectrum of species i , $P_{ii}(\omega)$, can be calculated by taking the Fourier transform of the Langevin equations Eq. (15):

$$P_{ii'}(\omega) = \langle \tilde{\xi}_i(\omega) \tilde{\xi}_{i'}(-\omega) \rangle \quad (16)$$

with $i' = i$, and its Fourier transform gives the autocorrelation function. The phase difference between the fluctuation fields is defined as

$$\theta_{ii'}(\omega) = \tan^{-1} \frac{\text{Im}[P_{ii'}(\omega)]}{\text{Re}[P_{ii'}(\omega)]}. \quad (17)$$

For example, the phase difference between total prey and the predator, $\theta_{(W+D)P}$, can be calculated from $P_{(W+D)P}(\omega) = \langle (\tilde{\xi}_W(\omega) + \tilde{\xi}_D(\omega)) \tilde{\xi}_P(-\omega) \rangle = P_{WP}(\omega) + P_{DP}(\omega)$, which has the form of

$$P_{(W+D)P}(\omega) = \frac{\beta_6 \omega^6 + \beta_4 \omega^4 + \beta_2 \omega^2 + \beta_0}{\omega^8 + \alpha_6 \omega^6 + \alpha_4 \omega^4 + \alpha_2 \omega^2 + \alpha_0} \quad (18)$$

with a tail proportional to ω^{-2} . The spectrum of phase difference between the predator and the total prey can be calculated from Eq. (17).

The autocorrelation function, $P_{ii}(\omega)$, peaks at the resonant frequency which is smaller than the oscillation frequency of the deterministic solution because of the renormalization by the white noise in Eq. (15) [34]. The longer period is the result of existence of the defended prey that causes the delay of the regrowth of the wild-type prey and the predator.

Results of analytic calculations and simulations based on ILM in Eq. (1) are shown in Fig. 1. We use the Gillespie algorithm [51] for stochastic simulations and introduce random mutation between prey sub-populations. We tried to simulate the experimental results of the rotifer-algae system done in a chemostat environment, where the control parameters are the nutrient concentration in flow media, $\phi_{N,\max}$, and the dilution rate, b . The natural degradation rates of the wild-type prey and predator are assumed to be much slower than the dilution rate, and therefore $b \approx d_R \approx d_W < d_D$ (the defended

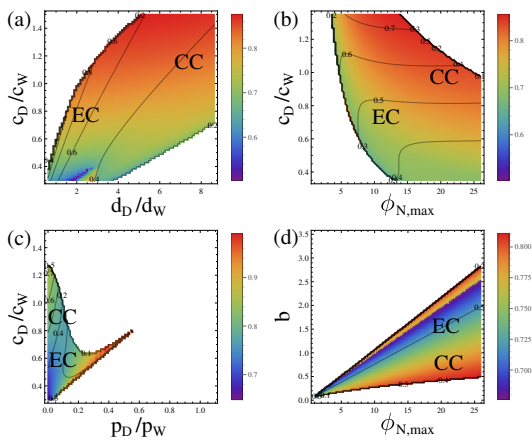


FIG. 2. Phase diagrams calculated from SILM with respect to ratio of prey reproduction rate (c_D/c_W), ratio of predation rate (p_D/p_W), the maximum nutrient concentration ($\phi_{N,\max}$) and the dilution rate (b). The colorful and white regions respectively correspond to coexistence of the two types of prey and extinction of the defended prey (D). The color legend represents the predicted phase difference between the wild-type prey and the defended prey (θ_{WD}), in units of π . The contours are the estimated ratios of population fluctuations to mean-field solutions; when fluctuations are larger than mean-field solutions, the dynamics is under high risk of extinction. Except for the axis specified in each diagram, the parameters in calculations are $V = 300$, $c_W = 1$, $p_W = 1$, $c_D/c_W = 0.8$, $p_D/p_W = 0.01$, $r_D/r_W = 3.5$, $\phi_{N,\max} = 16$, and $b = 0.6$.

prey is less healthy). In Fig. 1(a), at first there are only the wild-type prey and the predator in the system, and the dynamics exhibits normal cycles where the predator lags behind the prey by $\pi/2$. When predation pressure is high, around $t \sim 400$, a mutation has given rise to a defended prey population which subsequently adapts to dominate the population and cause additional delay in growth of the wild-type prey and the predator, leading to evolutionary cycles with π phase shift between the total prey and the predator. Fig. 1(b) shows an example of cryptic cycles, where the defended prey has similar reproduction rate as that of the wild-type prey, *i.e.* $c_D \lesssim c_W$, and the defended prey can advance the wild-type prey by nearly π and thus the total prey population is suppressed. The quasicycle calculations in Fig. 1(f)-(h) for power spectrum and phase spectrum in Eq. (16) with $i = i'$ and Eq. (18) well predict the simulation results in Fig. 1(c)-(e).

The phase diagram is usually studied by linear stability analysis of the mean field equations in Eq. (11). To reduce the dimension of parameter space, variables are rescaled to be dimensionless: $\tilde{t} \equiv bt$, $\tilde{d}_i \equiv d_i/b$, $\tilde{\phi}_i \equiv \phi_i/\phi_{N,\max}$, $\tilde{c}_i \equiv c_i\phi_{N,\max}/b$ and $\tilde{p}_i \equiv p_i\phi_{N,\max}/b$. However, this rescaling is rather subtle in stochastic calculations. For example, matrix **A** and **B** from Eq. (15) scale with $1/\phi_{N,\max}$ as mean-fields ϕ_i , but γ in Eq. (15) rescales

with $1/\sqrt{\phi_{N,\max}}$, resulting in

$$\frac{\xi_i}{\phi_i} \sim \frac{1}{\sqrt{\phi_{N,\max}}} \frac{\tilde{\xi}_i}{\tilde{\phi}_i} \quad (19)$$

where $\tilde{\xi}_i$ are the rescaled demographic noise fields. Therefore, for two stochastic individual-level models with same mean-field limit after rescaling, demographic fluctuations are more important in the model with smaller nutrient carrying capacity $V\phi_{N,\max}$. Thus neglecting fluctuations as in the conventional rescaling for mean-field equations can cause unphysical predictions for the phase diagram. To avoid such situation, we examine the stability of solutions by comparing the amplitude of population fluctuations, which is approximated by their auto-correlation functions, with their mean fields.

Fig. 2 shows the calculated phase diagrams of SILM in Eq. (1). In Fig. 2(a), due to the cost for defense, the defended prey have inferior reproduction rate ($c_D < c_W$) and are unhealthier than the wild-type prey ($d_D > d_W$), leading to evolutionary cycles (EC). When the cost of reproduction is low, cryptic cycles (CC) can occur, where $\theta_{WD} \approx \pi$. If the defended prey has a moderate reproduction rate, it is possible to have a correspondingly high death rate, and thus the fluctuations of prey are suppressed relative to the wild-type prey, causing the dynamics to be cryptic. In Fig. 2(b), under high concentration of nutrient ($\phi_{N,\max}$), the defended prey are more likely to grow and dominate the system, which causes the wild-type prey to experience a greater phase lag than the defended prey, and the dynamics tends towards a completely cryptic cycle. In Fig. 2(c), if the predation rate of the defended prey being hunted by the predator p_D is low, then the higher reproduction rate c_D can lead to more phase delay and thus gives cryptic cycles. When p_D increases, the predator has greater food resource available from the defended prey, yielding a larger population, which then consumes more of the wild-type prey; this in turn reduces the wild-type prey population and leads to the dominance of the defended prey. In such a situation, the wild-type prey experiences a greater phase delay (nearly π) behind the defended prey, but the wild-type prey population is too small to cancel out the fluctuations of the defended prey population, and thus the dynamics cannot be characterized as cryptic. Thus, by considering the amplitude of stochastic fluctuations, our result in Fig. 2(c) predicts a similar but slightly different phase diagram to Fig. 3 in [39]. In Fig. 2(d), under small dilution rate b , *i.e.* slow supplement of the nutrient and low reduce rate from dilution, although both subpopulations of the prey have low reproduction, the wild-type prey population decreases more due to predation while the defended prey has a greater chance to compete for nutrient, and thus the system is more likely to show cryptic cycles.

In summary, we have shown that a generic stochastic individual-level model can yield rapid evolution phenomena. We expect this description to be especially useful

to study the transition to rapid evolution from normal cycles, since before the transition the mutant prey have

extreme low population and are highly localized, amplifying the effects of demographic stochasticity and the role of spatiotemporal patterns.

-
- [1] S. A. Levin, *Ecology* **73**, pp. 1943 (1992).
- [2] J. Bascompte and R. V. Solé, *Trends in Ecology & Evolution* **10**, 361 (1995).
- [3] M. Pascual and S. A. Levin, *Ecology* **80**, 2225 (1999).
- [4] M. Pascual, P. Mazzega, and S. A. Levin, *Ecology* **82**, pp. 2357 (2001).
- [5] N. Goldenfeld and C. Woese, *Annu. Rev. Condens. Matter Phys.* **2**, 375 (2011).
- [6] J. Chave, *Ecology Letters* **16**, 4 (2013).
- [7] C. Elton and M. Nicholson, *Journal of Animal Ecology* **11**, 215 (1942).
- [8] M. Pineda-Krch, H. J. Blok, U. Dieckmann, and M. Doebeli, *Oikos* **116**, 53 (2007).
- [9] J. A. Bonachela, M. A. Muñoz, and S. A. Levin, *Journal of Statistical Physics* **148**, 724 (2012).
- [10] M. B. Bonsall and A. Hastings, *Journal of Animal Ecology* **73**, 1043 (2004).
- [11] D. L. DeAngelis and W. M. Mooij, *Annual Review of Ecology, Evolution, and Systematics*, 147 (2005).
- [12] E. Meron, *Ecological Modelling* **234**, 70 (2012).
- [13] A. Liebhold, W. D. Koenig, and O. N. Bjørnstad, *Annual Review of Ecology, Evolution, and Systematics*, 467 (2004).
- [14] H. Malchow, F. M. Hilker, I. Siekmann, S. V. Petrovskii, and A. B. Medvinsky, in *Aspects of Mathematical Modelling* (Springer, 2008) pp. 1–26.
- [15] R. HilleRisLambers, M. Rietkerk, F. van den Bosch, H. H. Prins, and H. de Kroon, *Ecology* **82**, 50 (2001).
- [16] B. Blasius, A. Huppert, and L. Stone, *Nature* **399**, 354 (1999).
- [17] S. Levin and L. Segel, *Nature* **259**, 659 (1976).
- [18] S. Kinast, Y. R. Zelnik, G. Bel, and E. Meron, *Physical review letters* **112**, 078701 (2014).
- [19] T. Butler and N. Goldenfeld, *Phys. Rev. E Rapid Communications* **80**, 030902 (2009).
- [20] T. Butler and N. Goldenfeld, *Phys. Rev. E* **84**, 011112 (2011).
- [21] J. A. Sherratt, M. A. Lewis, and A. C. Fowler, *Proceedings of the National Academy of Sciences* **92**, 2524 (1995).
- [22] M. Mobilia, I. Georgiev, and U. Tuber, *Journal of Statistical Physics* **128**, 447 (2007).
- [23] Q.-X. Liu, A. Doelman, V. Rottschfer, M. de Jager, P. M. J. Herman, M. Rietkerk, and J. van de Koppel, *Proceedings of the National Academy of Sciences* **110**, 11905 (2013).
- [24] A. J. McKane and T. J. Newman, *Phys. Rev. Lett.* **94**, 218102 (2005).
- [25] A. J. Black and A. J. McKane, *Trends in ecology & evolution* **27**, 337 (2012).
- [26] C. A. Lugo and A. J. McKane, *Physical Review E* **78**, 051911 (2008).
- [27] T. Butler and D. Reynolds, *Phys. Rev. E* **79**, 032901 (2009).
- [28] N. van Kampen, *Canadian Journal of Physics* **39**, 551 (1961).
- [29] M. Doi, *Journal of Physics A: Mathematical and General* **9**, 1465 (1976).
- [30] P. Grassberger and M. Scheunert, *Fortschritte der Physik* **28**, 547 (1980).
- [31] A. Mikhailov, *Physics letters A* **85**, 214 (1981).
- [32] N. Goldenfeld, *Journal of Physics A Mathematical General* **17**, 2807 (1984).
- [33] D. C. Mattis and M. L. Glasser, *Reviews of Modern Physics* **70**, 979 (1998).
- [34] U. C. Täuber, *Journal of Physics A: Mathematical and Theoretical* **45**, 405002 (2012).
- [35] A. A. Berryman, *Ecology* **73**, 1530 (1992).
- [36] J. N. Thompson, *Trends in Ecology & Evolution* **13**, 329 (1998).
- [37] G. F. Fussmann, S. P. Ellner, K. W. Shertzer, and N. G. Hairston Jr., *Science* **290**, 1358 (2000).
- [38] T. Yoshida, L. E. Jones, S. P. Ellner, G. F. Fussmann, and N. G. Hairston, *Nature* **424**, 303 (2003).
- [39] T. Yoshida, S. P. Ellner, L. E. Jones, B. J. M. Bohannan, R. E. Lenski, and N. G. Hairston, Jr., *PLoS Biol* **5**, e235 (2007).
- [40] L. Jones and S. Ellner, *Journal of Mathematical Biology* **55**, 541 (2007).
- [41] L. Becks, S. P. Ellner, L. E. Jones, and N. G. Hairston Jr, *Ecology Letters* **13**, 989 (2010).
- [42] L. Becks, S. P. Ellner, L. E. Jones, and N. G. Hairston, *Ecology Letters* **15**, 492 (2012).
- [43] B. J. M. Bohannan and R. E. Lenski, *Ecology* **78**, 2303 (1997).
- [44] S. P. Ellner, *Functional Ecology* **27**, 1087 (2013).
- [45] K. W. Shertzer, S. P. Ellner, G. F. Fussmann, and N. G. Hairston, *Journal of Animal Ecology* **71**, 802 (2002).
- [46] A. Yamauchi and N. Yamamura, *Ecology* **86**, 2513 (2005).
- [47] M. H. Cortez and S. P. Ellner, *The American Naturalist* **176**, E109 (2010).
- [48] A. Mougi, *Theoretical Population Biology* **81**, 113 (2012).
- [49] M. Yamamichi, T. Yoshida, and A. Sasaki, *The American Naturalist* **178**, 287 (2011).
- [50] A. Mougi, *Journal of Theoretical Biology* **305**, 96 (2012).
- [51] D. T. Gillespie, *The Journal of Physical Chemistry* **81**, 2340 (1977).